arXiv:1602.04582v1 [astro-ph.SR] 15 Feb 2016

Spectral atlas of two peculiar supergiants: MWC 314 and IRC +10420

E.L. Chentsov, V.G. Klochkova, and N.S. Tavolganskaya

Special Astrophysical Observatory RAS, Nizhnij Arkhyz, 369167 Russia

February 16, 2016

Abstract An atlas of spectra of the unique high luminosity objects MWC 314 and IRC +10420 taken with the CCD echelle spectrograph at the prime focus of the 6 m telescope of SAO is presented. About 320 emission and absorption features of stellar, circumstellar and interstellar nature are identified in the interval between 4790 and 7520 ÅÅ. Their relative intensities and radial velocities are given and the distinctions of their profiles are discussed.

1. Introduction

The purpose of the paper is two-fold: to represent in the graphical and tabulated forms the spectra which may prove to be helpful in the studies of various Be and Ae stars and to isolate the characteristic properties that have to be taken into account in constructing their photosphere (pseudophotosphere) and envelope models.

The spectra of MWC 314 and IRC +10420 are brought together for the following reasons.

– In spite of the fact that the sets of photospheric absorption lines in the objects and, accordingly, their spectral classes (given in Table 1) are different, their emission spectra bear resemblance to one another. In both cases one and the same permitted and forbidden components of iron group ion lines dominate. The profiles of these lines are, however, different. When going from MWC 314 to IRC +10420, some emission lines get narrower, others acquire absorption components or even transform fully to absorptions. This helps in identification, especially in clearing up the composition of blends.

– The nature and evolutionary status of the stars are not quite clear. Both of them are super- or even hypergiants, they are surrounded with envelopes of complex structure and kinematics (Miroshnichenko et al., 1998, Klochkova et al., 1997, Oudmaijer, 1998).

– They are of value also for refining the structure of the Galaxy since they are close to each other on the sky, in the north-western part of Aquila (Table 1). This Milky Way region is deficient in bright O stars and supergiants since it corresponds to a direction between the local arm and the Car–Sgr arm.

2. Observational data

The spectra were obtained with the echelle spectrograph PFES (Panchuk et al., 1998) at the prime focus of the 6 m telescope of SAO RAS in 1997 (the dates of observations are listed in the last column of Table 1). The CCD used has 1160 × 1040 pixels, 16 × 16 microns each.

Table 1. Main data of the objects

Name	α, δ (2000)	l, b	V	Sp	Date
MWC 314	$19^h21^m34^s.1$	$49^o.6, +0^o.3$	$9^m.9$	B3	22.11.97
(V1429 Ag1)	$14^o52'56''$				
IRC +10420	$19^h26^m48^s.1$	$47^o.1, -2^o.5$	$11^m.0$	A5	19.05.97
(V1302 Ag1)	$11^o21'17''$				

The reduction of the echelle images was performed in the system ESO MIDAS. When taking positional measurements of the line profiles, a computer fit of their correct images to mirror ones was applied.

Eighteen orders spanning a wavelength interval from 4790 to 7520 ÅÅ are presented in the atlas. The mean spectral resolution limit is 0.5 Å. A thorium-argon hollow-cathode lamp was employed as a comparison spectrum. The dispersion curves are checked and corrected using the telluric lines O_2 and H_2O, which are well visible in Fig. 3. However, the remaining systematic error of the presented radial velocities may reach 2–3 km/s.

3. Spectroscopic specific characteristics of the objects

MWC 314 possesses all of the features of the B[e] supergiant (Lamers et al., 1998), but for the strong infrared excess. Along with the numerous permitted low-excitation emission lines, FeII, CrII, ScII and others, there are a few forbidden lines ([FeII], [CaII] and others) as well as strong emission H and HeI lines in the spectrum described in detail by Miroshnichenko et al. (1998). The lines HeI 5876 Å and 6678 Å and, possibly, H_β show P Cyg type profiles. The absorption component of the spectrum in the region accessible to us is represented by weak lines NII, AlIII, SII, NeI and others, which are typical of early subclasses of spectral class B.

By the likeness of the profiles and closeness of the radial velocities, the lines can be divided into several groups. The mean heliocentric velocity values for these groups are tabulated in Table 2 (the number of the lines used is indicated in column 2), while the typical profiles are shown in Fig. 1.

Table 2. Heliocentric radial velocities (km/s) for groups of lines in the spectra of MWC 314 22.11.97.

Group of lines	n	Vr
Emissions:		
FeII, CrII, ScII, MgI (r < 1.5)	30	40
NaI	2	37:
FeII (r > 1.7); [FeII], [CaII]	7	33
HeI	4	30:
SiII	3	16
H_β		47
Absorptions:		
SII, NII, NeI	13	81
HeI	2	> -800:, -350
NaI (I.S.)	2	13
DIB	16	3

Apparently, all metallic emission lines are two-peaked. The radial velocities measured from the profile as a whole are presented in the 1st and 3d lines of Table 2. However, more than half

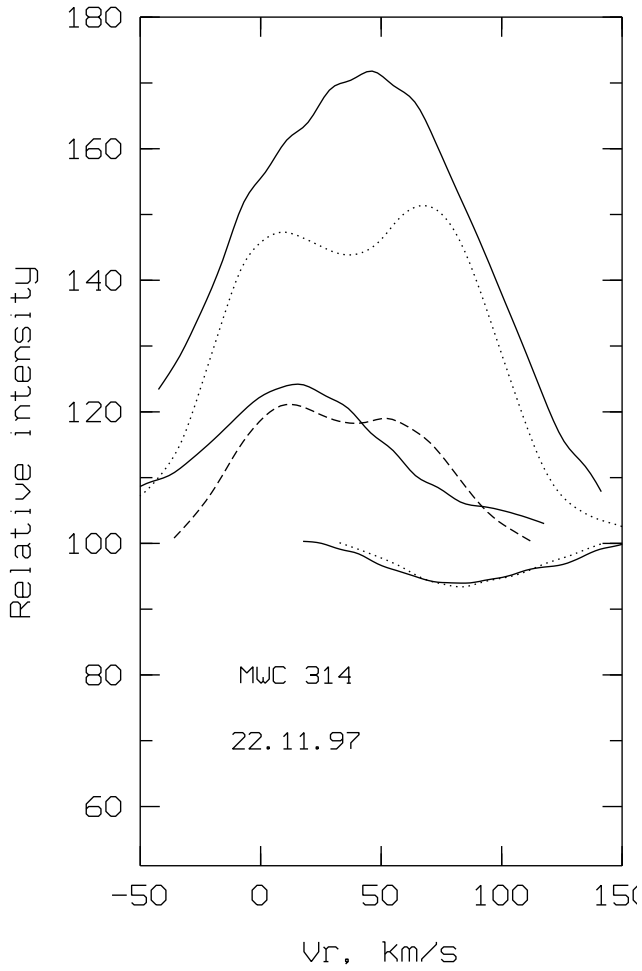

Figure 1. Typical line profiles in the spectrum of MWC 314. From top to bottom: emissions FeII(42) 4923, FeII(40) 6432 (dotted line), SiII(2) 6347, [FeII]14F 7155 (dashed line); absorption NeI(1) 6142 and 6402 (dotted line).

of the lines are intensive enough and not distorted by blending too much to allow radial velocity measurements from the blue and red peaks separately. Their values for the emission lines of moderate intensity are close to 2 and 72 km/s, respectively. The blue peak is more stable: as can be seen from Fig. 1, it preserves its position when going both to stronger permitted lines and to weaker forbidden lines. The red component in the lines [FeII] is displaced to 52 km/s, while the displacement in the strongest FeII lines is as large as 45 km/s, which causes shift of the line as a whole. In the emission line SiII, it is likely to merge (at least, with our resolution) with the blue component, or gets lost on the flat red wing.

The weakest emission lines of HeI show radial velocities of about 20 km/s; in stronger ones, they reach the value indicated in Table 2, 30 km/s. The velocity from H_β is still higher. This may result from strengthening of the wind absorption components in these lines.

As regards the photospheric absorption lines, they are displaced redward with respect to the emission lines, however, no mutual shifts falling outside the error limits are detected inside this group.

The spectrum of IRC+10420 demonstrates a still wider variety of the line profile shapes and their differential shifts. The transition from absorptions to emissions in it is represented by numerous lines with inverse P Cyg profiles (Fig. 2).

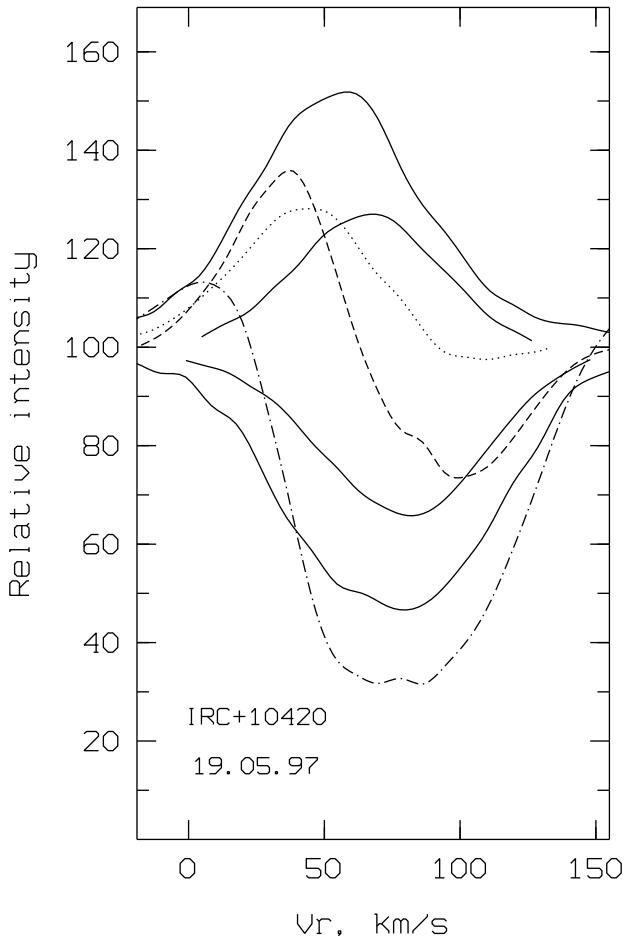

Figure 2. Typical line profiles in the spectrum of IRC +10420. From top to bottom: emissions FeII(40) 6432 and [FeII]14F 7155; emission-absorptions FeII(74) 6456 (dashed line), FeII(42) 5169 (dashed-dotted line) and FeII(74) 6416 (dotted line); absorptions NI(3) 7468 and SiII(2) 6347.

For the forbidden lines, the radial velocity is practically independent of line intensity: 64 km/s from weak [FeII] and 66 km/s from strong [CaII]. The value given in the 1st line of Table 3 is obtained also from measuring the lower parts of the hydrogen emission line profiles. Weak absorption lines of HeI and some others formed in the deepest and accessible to us layers of the atmospheres of the stars also yield a close value (4th line of Table 3).

Stronger lines free from obvious distortions by emission details (SiII, NI) are shifted redward with respect to the forbidden lines. This, certainly, refers to the absorption components of the inverse P Cyg profiles in which the shift is proportional to the relative intensity. For the deepest depressions, the velocity will be equal to that from the absorption components of the hydrogen lines (5th and 6th lines of Table 3), whereas for the shallowest of them it will reach 90 km/s (9th line of Table 3). The blueward shift of the emission lines is greater the deeper are the absorptions accompanying them. In the 3rd line of Table 3 is given the mean velocity value, measured from the emission peak, for the group of lines with the weakest absorptions. As they get more intensive, the velocity drops from 40 to 10 km/s. The shift is, however, preserved also in the lines that look like pure emission lines (2nd line of Table 3).

It is unclear to which group of lines the circumstellar components of the doublet NaI(1) belong. Possibly these are extension of the series of pure absorption lines arranged in the order

Table 3. Heliocentric radial velocities (km/s) for groups of lines in the spectra of IRC +10420 19.05.97.

Group of lines	n	Vr
Emissions:		
[FeII], [CaII], [OI]	8	65
FeII(40.46), MnII	12	54
FeII (48, 49, 74) ($r_{abs} > 0.8$)	7	40
Absorptions:		
HeI, SiII(4,5), OI	4	67
FeII (42, 48, 49) ($r < 0.5$)	5	70
$H_{\alpha,\beta}$	2	71
SiII(2)	2	76
NI	3	80
FeII(74), TiII, CrII, ScII ($r > 0.75$)	10	90
NaI	2	90
NaI (I.S.)	2	11
DIB	15	2

of increasing velocity: SiII(2) — 76 km/s, NI(3) — 80 km/s, NaI(1) — 90 km/s. However, it is not improbable that we see the absorption components of the inverse P Cyg profiles whose emission components are overlapped by interstellar absorption lines.

Spectroscopy of IRC +10420 suggests that envelope surrounding the object is inhomogeneous and non-stationary. The multilayer structure and, possibly, the non-sphericity of the envelope, apart from the existence of different shapes of the profiles shows up also in the deformation of broad absorption lines by local depressions. Some of them can be seen in Fig. 2.

The variations of line intensities and profiles of the envelope from 1992 to 1997 (from the spectra taken with the 6 m telescope of SAO and from Oudmaijer's (1995) data) were not of systematic character. They manifest themselves most clearly in the lines with inverse P Cyg profiles: the general gradient in intensity would change, i.e. both emission and absorption would be either intensified or alternated at a time. Apparently, the evolutionarily significant variation of the spectra, which reflects the elevation of the photosphere (or pseudophotosphere) temperature, continued: the line HeI 5876 Å intensified, traces of the absorption lines HeI 4921 Å and 5015 Å appeared.

Note that there are rather deep and sharp absorption lines in the spectrum of IRC +10420 at $\lambda\lambda$ 5693, 6282, 6287 and 6289 ÅÅ. Their nature has so far not been established.

The interstellar lines and diffusion bands are strong in the spectra of the two stars. Their equivalent widths and radial velocities (the last lines of Tables 2 and 3) are indicative of the great distance of both objects. However, taking account of the interstellar extinction, even adopting the limiting luminosity, it is difficult to estimate distances at which the observed stellar velocities would be accounted for by the Galactic rotation alone. For the longitude in question, the heliocentric radial velocities of disk objects do not exceed 50–55 km/s (Avedisova, 1996). This maximum value corresponds to a distance of about 7 kpc. Meanwhile, a distance of 2.5 kpc for MWC 314 requires $M_V \approx -8^m$, and for IRC +10420 even -9^m.

At the same time, it has to be seen which of the values presented in Tables 2 and 3 could be thought to be the velocities of the centres of mass of the stars. In the case of MWC 314, the most appropriate velocity seems to be the one found from the two-peaked emission lines of moderate intensity, which, possibly, form in the gaseous ring surrounding the star. This velocity does not go over the limit indicated above, but it disagrees with the velocity given by photospheric

absorption lines. There is no such a discrepancy in IRC +10420, but the velocity turns out to run over the limit.

To solve the above-mentioned matters, further observations, preferably with a higher spectral and temporal resolution, are needed.

4. The atlas and list of the identified lines

In Fig. 3 the spectra of the objects are presented graphically as relationships between relative intensity and wavelengths in the interval 4790–7520 ÅÅ. Its fragments correspond to spectral orders. There are little gaps only between the last three orders. The spectra are displaced along the horizontal axis so as its marking should correspond to the laboratory wavelengths for the groups of lines showing the radial velocity which correspond assumingly to the centre of mass of the star. For MWC 314 these are the emission lines of FeII and others (1st line of Table 2), for IRC +10420 the emission lines [FeII] and others and absorption lines of HeI and others (1st and 4th lines of Table 3, respectively).

In the atlas are shown the strongest lines which are present in the spectra of both stars and the diffusion interstellar bands. For IRC +10420, the dots mark defects.

Table 4 contains the identification of the lines (column 1), their laboratory wavelengths used in the estimation of radial velocities (column 2), re intensities of the profile extrema (columns 3, 5), and radial velocities of individual lines or their components in km/s (columns 4, 6).

A total of 320 features of stellar (possibly, circumstellar) and interstellar nature were identified. The telluric lines were not identified. The individual lines or blends are separated by the skips of the lines.

References

Avedisova V.A., 1996, Astron. Let. **22**, 497

Klochkova V.G., Chentsov E.L., Panchuk V.E., 1997, Mon. Not. R. Astron. Soc. **292**, 19

Lamers H.J.G.L.M., Zickgraph F-J., Winter D. de, Houziaux L., Zorec J., 1998, Astron and Astrophys. **340**, 117

Miroshnichenko A.S., Fremat Y., Houziaux L., Andrillat Y., Chentsov E.L., Klochkova V.G., 1998, Astron and Astrophys. Suppl. **131**, 469

Oudmaiyer R.D., 1995, PhD thesis, Univ. Groningen

Oudmaiyer R.D., 1998, Astron and Astrophys. Suppl. **129**, 541

Panchuk V.E., Najdenov I.D., Klochkova V.G., Ivanchuk A.B., Yermakov S.V., Murzin V.A., 1998, Bull. Spec. Astrophys. Observ **44**, 127

Table 4. Depths (r) and values of heliocentric radial velocity (V_r) measured for individual lines in spectra of stars studied

Ident	λ, Å	MWC 314		IRC +10420	
		r	Vr	r	Vr
1	2	3	4	5	6
[FeII] 4F	4798.3	1.06		1.11:	
TiII (17)	4798.53				
TiII (92)	4805.09	1.12	43:	0.75:	
CrII (30)	4812.34	1.07:	40:	0.87:	
[FeII] 20F	4814.53	1.06:		1.09:	
SII (9)	4815.52	0.90	73		
CrII (30)	4824.14	1.20	41	0.64	78:
FeII (30)	4825.72	1.08:		1.06:	
FeII (30)	4833.20	1.07	42:	1.06:	
CrII (30)	4836.22	1.08	43	1.06:	25:
				0.90:	92:
FeII (30)	4840.00	1.04:	42:		
CrII (30)	4848.25	1.15	39	1.09	25:
				0.66	95:
CrII (30)	4856.19			0.88	86:
H_β	4861.33	8.2	47	2.16	6
				0.47	72
				1.34	145:
CrII (30)	4864.32			0.68	80
FeII (25)	4871.27	1.04	41	0.91:	
TiII (114)	4874.02	1.03:		0.82	80:
CrII (30)	4876.40	1.06:		1.11:	35:
				0.64	88
DIB	4881.83				
CrII (30)	4884.60	1.03			
SII (15)	4885.60	0.93:			
[FeII] 4F	4889.62	1.05:	25:	1.15:	55:

1	2	3	4	5	6
FeII (36)	4893.81	1.07	35:	1.13:	55:
NII (1)	4895.11	0.95	78:		
YII (22)	4900.12			0.85	90:
[FeII] 20F	4905.34	1.04	21:		
TiII (114)	4911.19	1.07	37	1.08	0:
				0.85	70:
HeI (48)	4921.93	1.28:	15:	0.94:	
FeII (42)	4923.92	1.72	39	0.40	78
FeI (318)	4957.5:	1.03			
DIB	4963.96	0.96	10:		
[TiII] 23F	4982.73?	1.04		1.07:	
NII (24)	4987.37	0.97:	77:		
FeII (25)	4991.11	1.07:		1.14	88
FeII (36)	4993.35	1.26	45:	1.25	50:
FeII (25)	5000.73	1.20	37	1.03:	
NII (4)	5002.70	0.92	77:		
NII (24)	5007.33	0.88			
SII (7)	5009.54	0.88	69:		
HeI (4)	5015.68	1.77	25	0.88	
FeII (42)	5018.44	1.90	32	0.42	72
SII (1)	5027.19	0.97	79		
ScII (23)	5031.02	1.06	37:	0.77	80
SII (7)	5032.41	0.91	81		
FeII (36)	5036.93	1.05		1.06	75:
SiII (5)	5041.03	1.07	16:	0.92	
NII (4)	5045.10	0.94	83:		
HeI (47)	5047.74				
SiII (5)	5056.00	1.12	16:	0.80	68
TiII (113)	5072.29	1.09	44:	1.08:	35:
				0.89:	95:

1	2	3	4	5	6
NII (10)	5073.59	0.98	82:		
YII (20)	5087.42?			0.92:	
CrII (24)	5097.32	1.02:			
FeII (35)	5100.65	1.12	40	1.13	43
SII (7)	5103.30	0.93	79		
FeI(16,36)	5107.5:			1.08:	
[FeII] 19F	5111.63	1.05:	14:		
FeII (35)	5120.34	1.08	38:	1.08	30
TiII (86)	5129.14	1.15	41:	1.10:	2:
				0.85	75:
FeII (35)	5132.66	1.20	38	1.18	37:
FeII (35)	5136.79	1.09	40	1.08	38
FeII (35)	5146.11	1.11	39	1.13	44
FeII	5149.46?			0.93	
FeI (16)	5150.84			1.05:	50:
TiII (70)	5154.07	1.15	41	1.15	18
				0.73	78
[FeII] 19F	5158.78	1.16	34:	1.22	60
FeII (35)	5161.18	1.06	39:	1.04:	58:
MgI (2)	5167.33			1.12	30:
FeII (42)	5169.03	1.68	33	1.10	10:
				0.32	82
FeII (35)	5171.60			1.18:	65:
MgI (2)	5172.68	1.30:	37:	0.86:	80:
MgI (2)	5183.61	1.24	43	1.12	32
				0.78	86
TiII (86)	5185.90			1.15	29
				0.78	88
TiII (70)	5188.68	1.10	45:	1.08:	20
				0.55	86
FeII (49)	5197.57	1.46	40	1.28	27
				0.52	92

1	2	3	4	5	6
SII (39)	5201.15:	0.93	84:		
TiII (103)	5211.54	1.09		1.14	18
				0.93	: 78:
SII (39)	5212.61	0.94	81:		
[FeII] 19F	5220.06?			1.07:	59:
TiII (70)	5226.54	1.20	42:	1.10	14:
				0.70	72:
FeII (49)	5234.62	1.48	25	1.15:	5:
				0.60	72
CrII (43)	5237.32	1.17:	41:	1.02:	8:
				0.72	73
ScII (26)	5239.82	1.04:	42:	1.02:	18:
				0.90	72:
CrII (23)	5246.76	1.05	45:	1.03:	25:
				0.96:	90:
CrII (23)	5249.43	1.04:		1.03:	27:
FeII (49)	5254.93	1.26	46:	1.16	32
FeII (41)	5256.93	1.1:	37:	1.10	40:
FeII	5260.26?			0.91	
[FeII] 19F	5261.62	1.12		1.21	62
TiII (70)	5262.10				
FeII (48)	5264.80	1.20	42	1.14	28
				0.83	90
TiII (103)	5268.63	1.20		1.10:	
FeI (15)	5269.54				
[FeII] 18F	5273.36	1.10:			
CrII (49)	5274.99				
FeII (49)	5276.00	1.52		1.13	
				0.45	83
CrII (43)	5279.88	1.08	41:	1.09	32:
				0.91	87:
CrII (43)	5280.08				
FeII (41)	5284.10	1.35	42	1.29	35
				0.84	88
FeII	5291.67			0.96:	52:

1	2	3	4	5	6
CrII (24)	5305.85	1.09	50:	1.11	30
				0.94	: 92:
CrII (43)	5308.42	1.06	48:	1.12	30
				0.95:	87:
CrII (43)	5310.69			1.06	31
				0.98	: 82:
CrII (43)	5313.58	1.08:		1.08:	20:
				0.86	82
FeII(49,48)	5316.65:	1.82	32	1.26	16
				0.43	83
SII (38)	5320.70	0.92	80:		
FeII (49)	5325.56	1.25	40	1.21	28
				0.88	85
FeI (15)	5328.04	1.12		1.18	
FeI (37)	5328.53				
[FeII] 19F	5333.65			1.18:	
CrII (43)	5334.86	1.12	39:		
				0.87	72
TiII (69)	5336.79	1.20:	43:	1.18	
FeII (48)	5337.73				
FeII (49)	5346.56	1.04		1.05:	
FeII (48)	5362.86	1.43	35	1.22	28
				0.75	87
CrII (29)	5369.30?			1.03:	
FeI (15)	5371.49?	1.04:		1.05:	
[FeII] 19F	5376.47	1.04	24:	1.07:	70:
TiII (69)	5381.02	1.08	43	1.16	36
				0.93	95
TiII (80)	5396.30				
FeI (15)	5397.13	1.07:		1.13	35
DIB	5404.5:	0.95	7:	0.96:	2:
FeI (15)	5405.78	1.05:		1.03	56:
CrII (23)	5407.61	1.10:	45:	1.07	40:
[FeII] 17F	5412.65				
FeII (48)	5414.07	1.18	41	1.16	45:

1	2	3	4	5	6
TiII (69)	5418.78			1.10	44
				0.91	90
CrII (23)	5420.92	1.12	39:	1.10:	45:
FeII (49)	5425.25	1.32	42	1.18	40
				0.92	100
SII (6)	5428.64	0.98:	88:		
FeII (55)	5432.98	1.16	39	1.12	50:
FeI (15)	5446.91	1.02:		1.09	48
SII (6)	5453.81	0.90	81		
FeI (15)	5455.61	1.05		1.06:	48:
FeII	5466.92?	1.03:			
CrII (50)	5472.62	1.02:	43:		
SII (6)	5473.59	0.94	83:		
CrII (50)	5477.45				
CrII (50)	5478.36	1.10	36:	1.12	35:
				0.96	90:
DIB	5487.45	0.97:			
TiII (68)	5490.65	1.06		1.07	55:
FeI (15)	5497.52	1.04:	36:	1.03:	60:
CrII (50)	5502.08	1.12:		1.12:	
CrII (50)	5503.20				
FeII	5506.20			0.95:	55:
CrII (50)	5508.62	1.10:		1.06	43
CrII (23)	5510.70	1.04:		1.08	39
				0.98:	108:
FeII (56)	5525.11	1.08		1.10:	66:
ScII (31)	5526.81	1.15	41	1.12:	
				0.78	80
TiII (68)	5529.94	1.08	39	1.09	72
FeII (55)	5534.83	1.44	40	1.28	39
				0.81	97
DIB	5544.97	0.97:	-3:	0.96:	3:

1	2	3	4	5	6
SII (6)	5556.01	0.98	79:		
SII (6)	5564.96	0.95	79		
FeII	5567.84	1.05		1.07	63
[OI] 3F	5577.34				
SII (11)	5578.85	0.98	81:		
FeI (686)	5586.76	1.07		1.08	60:
FeII (55)	5591.37	1.05	38	1.04	65:
SII (11)	5606.11	0.95	78:		
DIB	5609.96	0.98	-3:	0.97	8:
FeI (686)	5615.64	1.03		1.04	45:
SII (11)	5616.63	0.98	76:		
FeI (686)	5624.54	1.02:		1.02:	
FeII (57)	5627.49	1.07	43	1.09	55:
SII(14,11)	5640.15:	0.93	77:		
ScII (29)	5640.98			1.04	36
				0.95	90
SII (6)	5645.62	0.98:	83:		
SII (14)	5646.98	0.93	81		
ScII (29)	5657.87	1.16	49	1.12	36
				0.86	95
SII (11)	5659.95	0.95:	90:		
YII (38)	5662.94			1.06	37
				0.94	93
SII (11)	5664.73	0.95:	81:		
NII (3)	5666.63	0.95	77:		
ScII (29)	5667.16	1.03:		1.04	35
				0.98:	86:
ScII (29)	5669.03	1.02:	38:	1.04	36
				0.95	88
NII (3)	5676.02	0.95	85:		
CrII (189)	5678.42	1.04:		1.03:	37:
				0.98:	100:
NII (3)	5679.56	0.91	89:		

1	2	3	4	5	6
ScII (29)	5684.19	1.07	43	1.08	42
				0.96	94:
NII (3)	5686.21	0.97	76		
	5687?			0.92	
NaI (6)	5688.21?			0.98	79:
	5692.5?			0.72	
AlIII(2)	5696.60	0.93	83:		
	5700.0?			0.91	
DIB	5705.1	0.94	6	0.96	5:
NII (3)	5710.77	0.96	83		
DIB	5719.43	0.98:	8:	0.98:	4:
AlIII(2)	5722.73	0.96	87:		
SiIII(4)	5739.73	0.95:	83:		
[NII] 3F	5754.8				
DIB	5766.25	0.96	-6:	0.96	0
DIB	5769.1	0.98:	4:		
DIB	5772.6	0.98	6:	0.98:	10:
DIB	5776.08	0.97		0.98:	
DIB	5780.41	0.67	7	0.74	4
DIB	5784.9	0.97	1:	0.97:	4:
DIB	5789.06	0.98			
DIB	5797.03	0.82	2:	0.75	8
DIB	5809.1:	0.97	4:	0.97:	6:
FeII (163)	5813.67?	1.06	40:	1.04:	38:
DIB	5818.85			0.98:	3:
FeII (182)	5835.49?	1.04		1.04	47:

1	2	3	4	5	6
DIB	5844.2	0.97		0.97	3
DIB	5849.79	0.93	6	0.87	2
NeI (6)	5852.49	0.97	85:		
HeI (11)	5875.72	0.85	-700:	0.91	65:
			-450:		
			-350:		
		4.00	28		
NaI (1)	5889.95	1.30	37:		
		0.06	13	0.09	10
				0.53	92:
NaI (1)	5895.92	1.25	36:		
		0.09	12	0.10	12
				0.54	86:
VII (98)	5928.86			1.05:	68:
FeII (182)	5952.52?	1.05:	46:	1.05	50:
SiII (4)	5957.56	0.95	75:	0.91	66
SiII (4)	5978.93	1.08	17	0.94:	75:
FeII (46)	5991.37	1.38	41	1.43	55
DIB	6004.9	0.97	6:	0.98:	-1:
DIB	6010.58	0.95	10:	0.98:	5:
DIB	6019.34	0.98:	8:	0.98:	
VII (97)	6028.26	1.05	37:	1.05	62:
VII (97)	6031.07	1.02:		1.03	60:
DIB	6037.56	0.97	-5:	0.98	: 4:
FeII (200)	6045.46	1.02	46:	1.03	
CrII (105)	6053.48	1.04	42:	1.05	50:
DIB	6065.38	0.98	5:	0.99:	
NeI (3)	6074.34	0.96	82:		
FeII (46)	6084.10	1.22	41	1.25	58
DIB	6089.75	0.96	0	0.97	3

1	2	3	4	5	6
NeI	6096.16	0.96	85:		
FeII (200)	6103.54	1.07	40	1.05	41:
DIB	6113.2			0.98:	
FeII (46)	6113.32	1.11	50:	1.14	64
FeII (46)	6116.05	1.05:		1.05	65:
MnII (13)	6122.43?	1.02:		1.03:	
FeII (46)	6129.71	1.08	40	1.10	60
FeI (169)	6136.61				
FeI (207)	6137.69	1.02:		1.08:	
BaII (2)	6141.72			1.05	42:
NeI (1)	6143.06	0.94	83		
FeII (74)	6147.74	1.55	41	1.26	40
FeII (74)	6149.25	1.35		1.20	46:
				0.96	98:
OI (10)	6156			0.95	
OI (10)	6158.18			0.95	65:
NeI (5)	6163.59	0.95	81		
FeII (200)	6175.15	1.05	40:	1.05:	
FeII (163)	6179.39	1.04	41:	1.05:	40:
FeI (169)	6191.56	1.03	40	1.06	65:
DIB	6195.95	0.93	4:	0.92	0
DIB	6203.06	0.87	8:	0.90	2
DIB	6212.2	0.97:	-10:	0.98:	-5:
FeII (34)	6219.54	1.04	47:	1.06	75:
FeII (34)	6229.34	1.07	51:	1.10	80:
FeI (207)	6230.74	1.04	33:	1.05:	75:
FeII (74)	6238.39	1.48	46:	1.27	42
FeII (74)	6239.95	1.20:		1.19	58
ScII (28)	6245.62			1.09	40
FeII (74)	6247.55	1.40	41	1.28	38

1	2	3	4	5	6
				0.81	100
FeI (169)	6252.56			1.03:	70:
	6259?	0.99:		0.97:	
DIB	6269.7	0.93		0.91	-1
FeI(342)	6270.24	1.06		1.09	65:
	6282.6?			0.85:	
DIB	6283.86	0.67	10	0.74	3
	6286.6?			0.81	
	6288.5?			0.79	
[OI] 1F	6300.3	1.04		1.21	66
[SIII] 3F	6312.06?	1.10	16:		
FeII	6317.99	1.25	41		
FeII (199)	6331.96	1.09	45	1.05	45:
NeI (1)	6334.43	0.97	73		
SiII (2)	6347.10	1.23	16	0.47	75
DIB	6353.5	0.96	2:	0.98	-8:
DIB	6362.4	0.98	3:	0.97	-5:
[OI] 1F	6363.78			1.05	67
FeII (74)	6369.47	1.38	53:	1.32	56
SiII (2)	6371.36	1.10:		0.59	78
DIB	6376.1	0.96	12:	0.97	3:
DIB	6379.2	0.86	1	0.85	2
FeII	6383.72	1.18	50:		
FeII	6385.45	1.1:		1.05:	
FeI (168)	6393.61	1.02:	40:	1.05	65:
FeI (816)	6400.01?	1.02:		1.03:	71:
NeI (1)	6402.25	0.92	83		
FeII (74)	6407.25	1.10	39	1.10	54
FeII (74)	6416.92	1.32	41	1.28	43
				0.98:	108:

1	2	3	4	5	6
DIB	6425.4	0.96	6:	0.97	9:
FeII (40)	6432.68	1.55	39	1.51	54
DIB	6439.4	0.97	2:	0.98	5:
[FeII] 15F	6440.4	1.02:	18:		
FeII	6442.95	1.05	35:		
DIB	6445.4	0.97		0.97	5:
FeII (199)	6446.43	1.05	48:	1.04	42:
DIB	6449.2			0.97	7:
FeII (74)	6456.38	1.60	40	1.35	38
				0.74	101
FeII (199)	6482.19	1.13	42	1.07	30:
				0.92	95:
TiII (91)	6491.57	1.15	43:	1.12:	40:
FeII	6491.67				
FeII	6493.03				
NeI (3)	6506.53	0.96	90:		
FeII (40)	6516.08	1.65	41	1.46	50:
H_α	6562.81			6.2	7
				1.93	70
				3.66	138
[NII] 1F	6583.6		10		
FeII	6586.70?		45:		
DIB	6597.39	0.98:		0.98:	
NeI (6)	6598.95		90:		
ScII (19)	6604.59	1.07:		1.06	45:
TiII (91)	6606.95			1.05	40:
DIB	6613.62	0.75	3	0.76	0
FeII (210)	6627.25	1.07	39	1.02:	
DIB	6660.65	0.94	5:	0.93	0
HeI (46)	6678.15	0.95	-400:		
			-290:		
			-115:		
		2.20	22		
TiII (112)	6680.26?			1.05	

1	2	3	4	5	6
DIB	6699.37	0.95	4:	0.95:	0:
DIB	6701.98	0.97	-8:	0.98:	6:
[SII] 2F	6717.0	1.03	27:		
TiII (112)	6717.91	1.02	35:	1.07	42:
DIB	6740.96	0.98:			
DIB	6770.05	0.98:	10:		
YII (26)	6795.41			1.03:	55:
DIB	6811.44	0.98	7:	0.99:	
DIB	6827.28	0.98	2:	0.99:	
[FeII] 31F	6829.01?	1.04	23:	1.06:	
DIB	6841.59	0.99		0.99:	
DIB	6843.44	0.98	0:	0.98:	3:
DIB	6852.9	0.98		0.98	
DIB	6860.02	0.98:		0.97	
DIB	6993.18	0.83	4:	0.88	8:
[TiII] 17F	6999.99?	1.06:	18:	1.05:	
HeI (10)	7065.2	0.95:			
		4.7	35		
DIB	7105.93	0.98	5:		
DIB	7119.94	0.97	-12:	0.96	
FeII (197)	7135.02?	1.10	38	1.02:	
				0.97:	
[FeII] 14F	7155.14	1.20	33:	1.27	65
TiII (101)	7214.73	1.05	41:	1.11	
FeII (73)	7222.39	1.1:		1.11:	
FeII (73)	7224.47	1.2:		1.22:	52:
HeI (45)	7281.35	1.70	20:		
[CaII] 1F	7291.46	1.60:	34:	2.40:	68
FeII (73)	7320.70	1.15:		1.22:	50:
[CaII] 1F	7323.88	1.40:	31:	2.23	65

1	2	3	4	5	6
MnII (4)	7330.54	1.05:		1.05:	
MnII (4)	7353.52	1.09:		1.09:	50:
TiII (101)	7355.46			1.10:	
	7378?	1.08		1.10	
[FeII] 14F	7388.16	1.11	15:	1.08:	
[VII] 4F	7411.9	1.06:	9:	1.07	53:
MnII (4)	7415.78	1.18	39:	1.17	50:
NI (3)	7423.64	1.06		0.82	80
MnII (4)	7432.27	1.06	37	1.11	52
NI (3)	7442.29	1.07	37:	0.77	80
FeII (73)	7449.33	1.18	40:	1.23	50
[FeII] 14F	7452.5	1.07:		1.10	68
FeII (73)	7462.39	1.32	39	1.36	44
				0.96:	105:
NI (3)	7468.31	1.07		0.66	80
FeII (72)	7479.69	1.10	40	1.10	50:
FeII	7495.63	1.07		1.02:	
FeII (73)	7515.79	1.27	37	1.39	

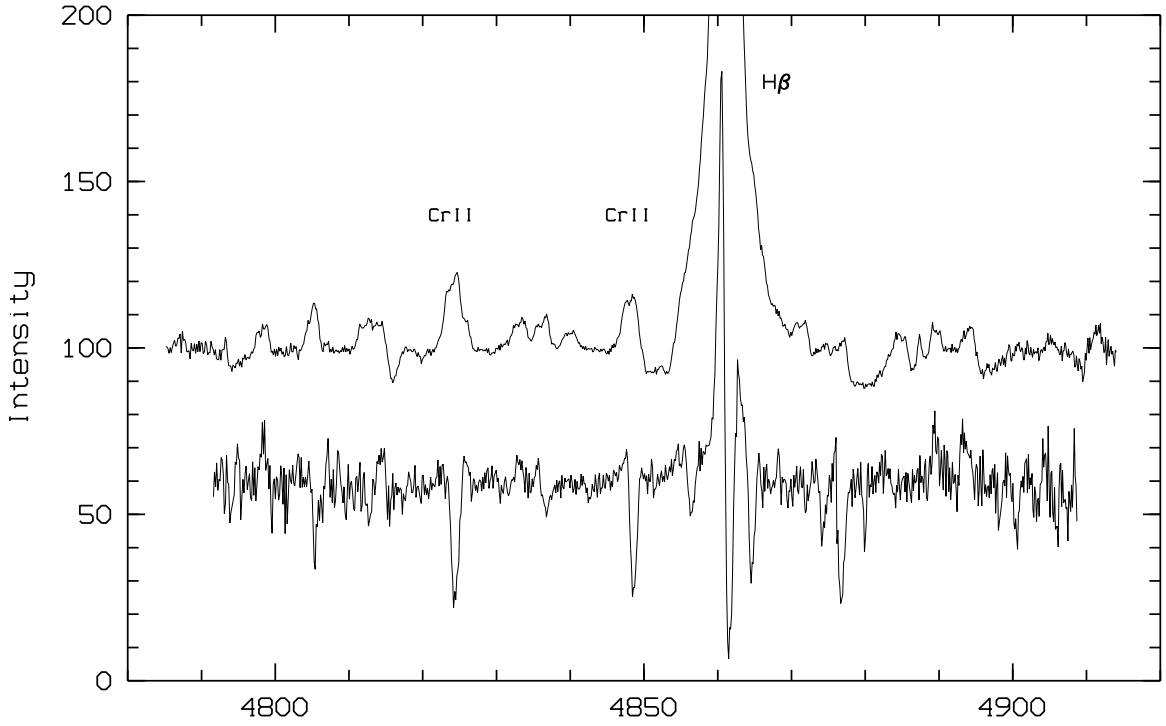

Figure 3. The spectra of MWC 314 (above) and IRC+10420 (lower). The wavelengths are given in Angstroms, the intensity is normalized to the continuum level

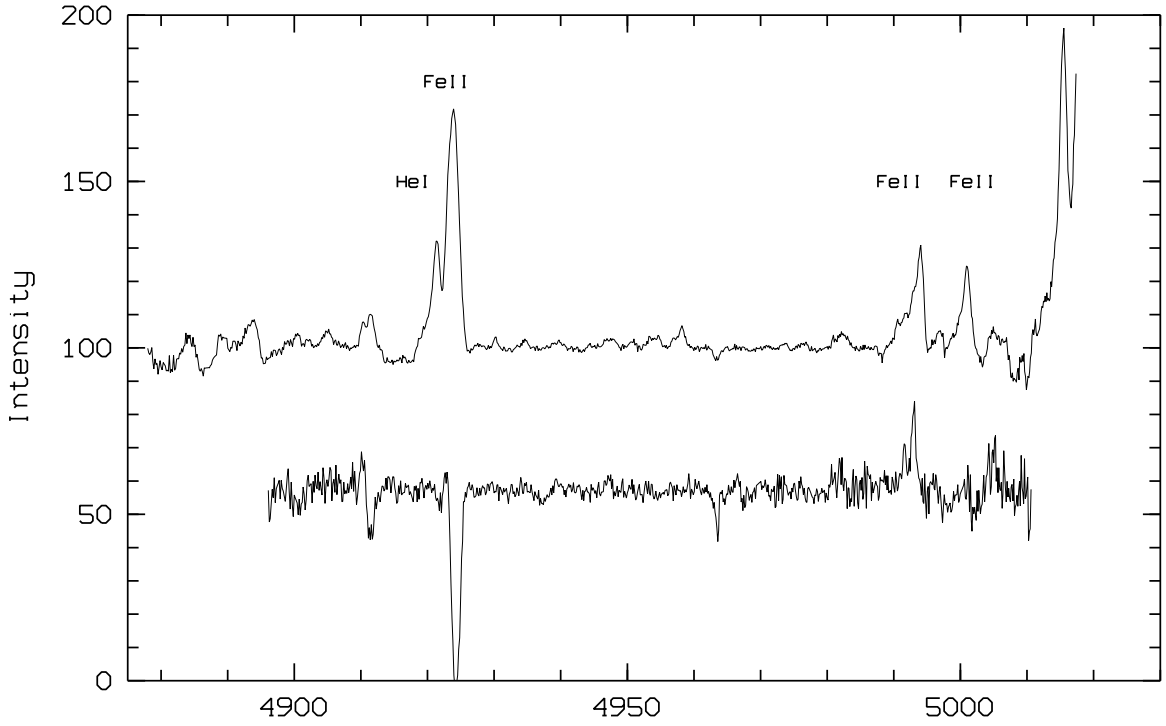

Figure 3.

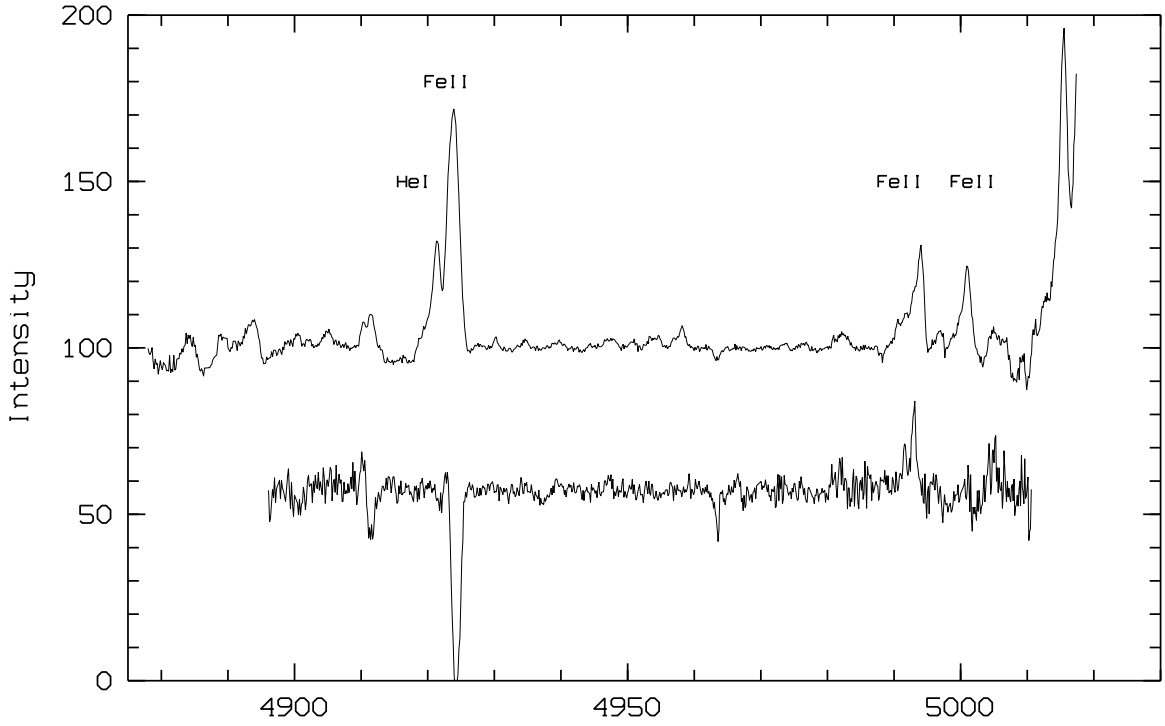

Figure 3.

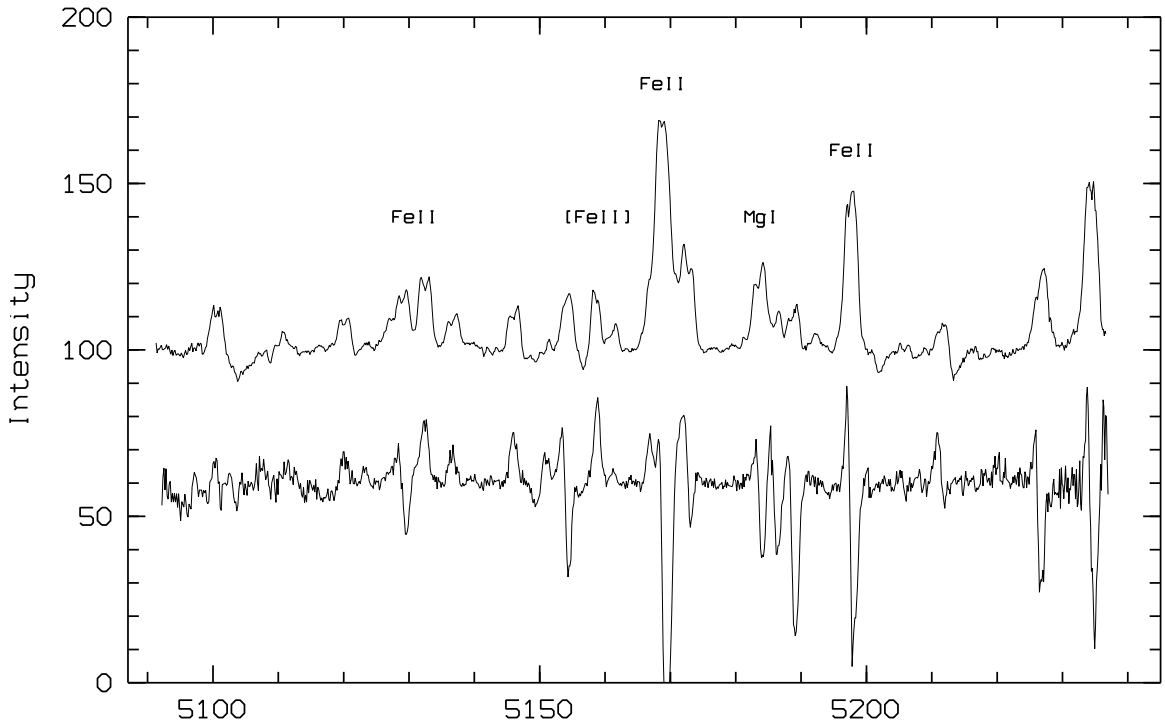

Figure 3.

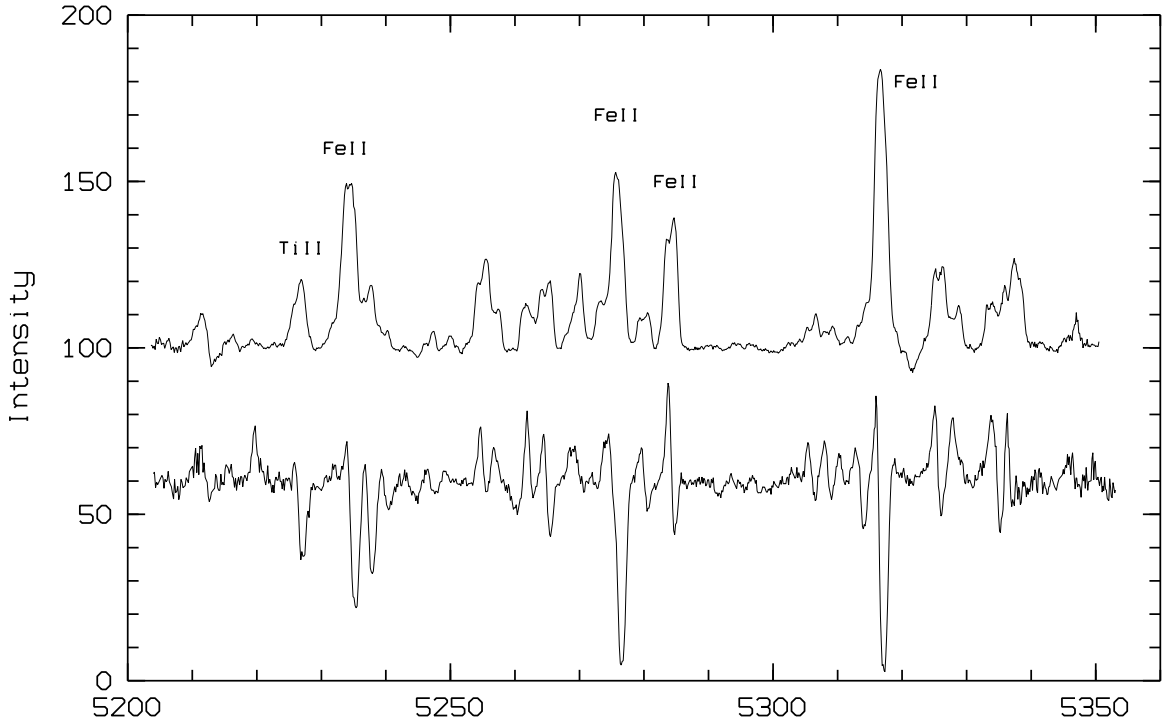

Figure 3.

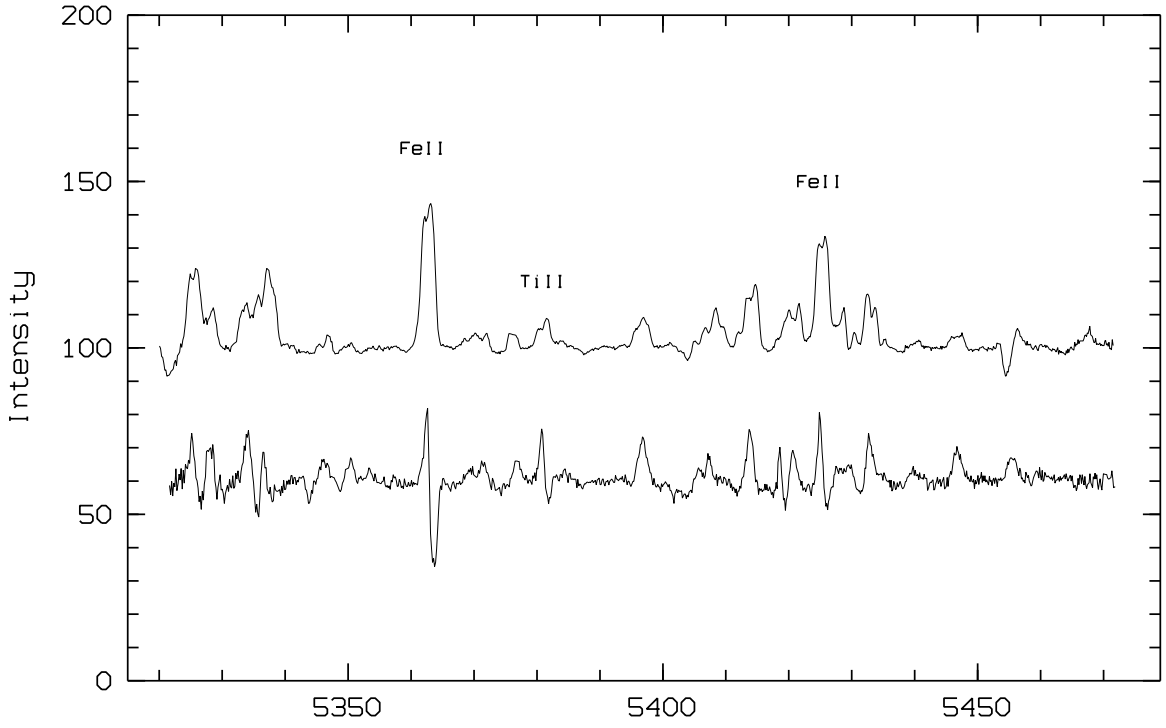

Figure 3.

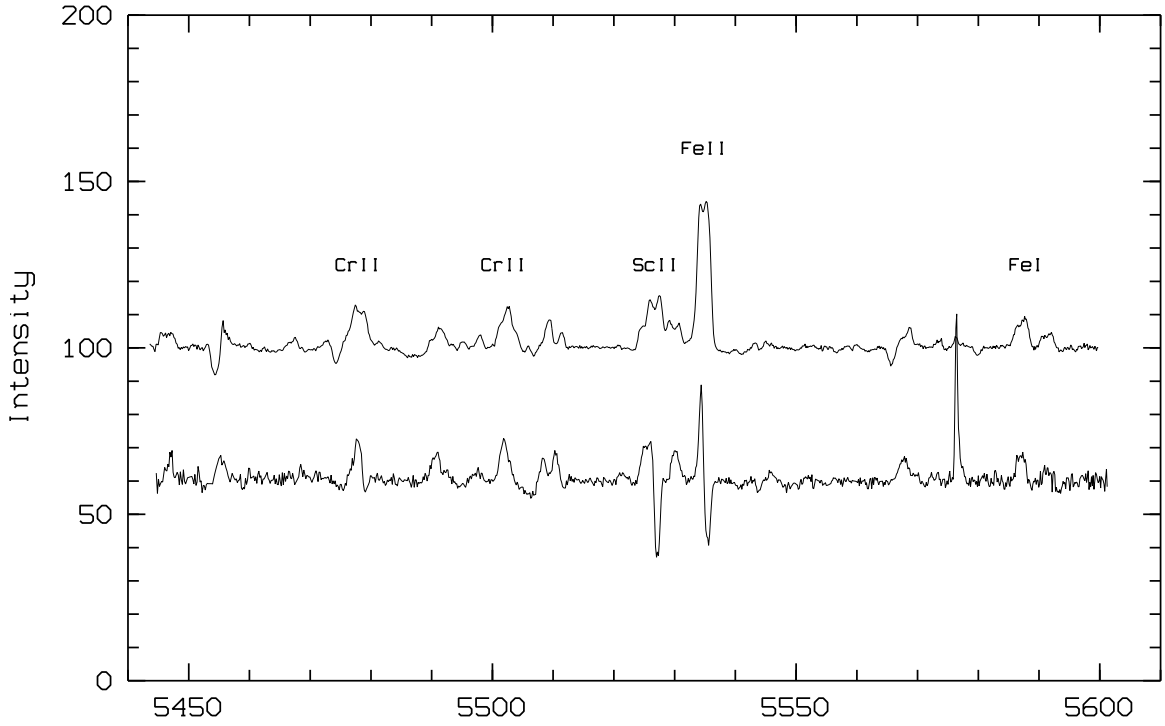

Figure 3.

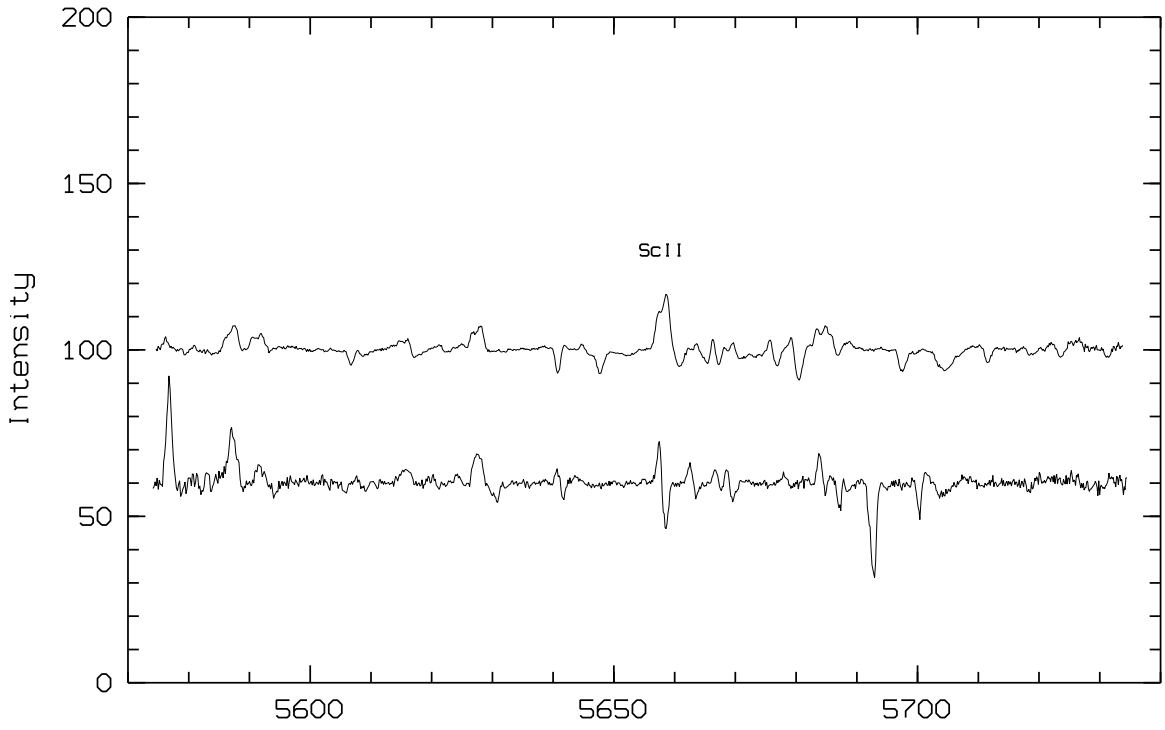

Figure 3.

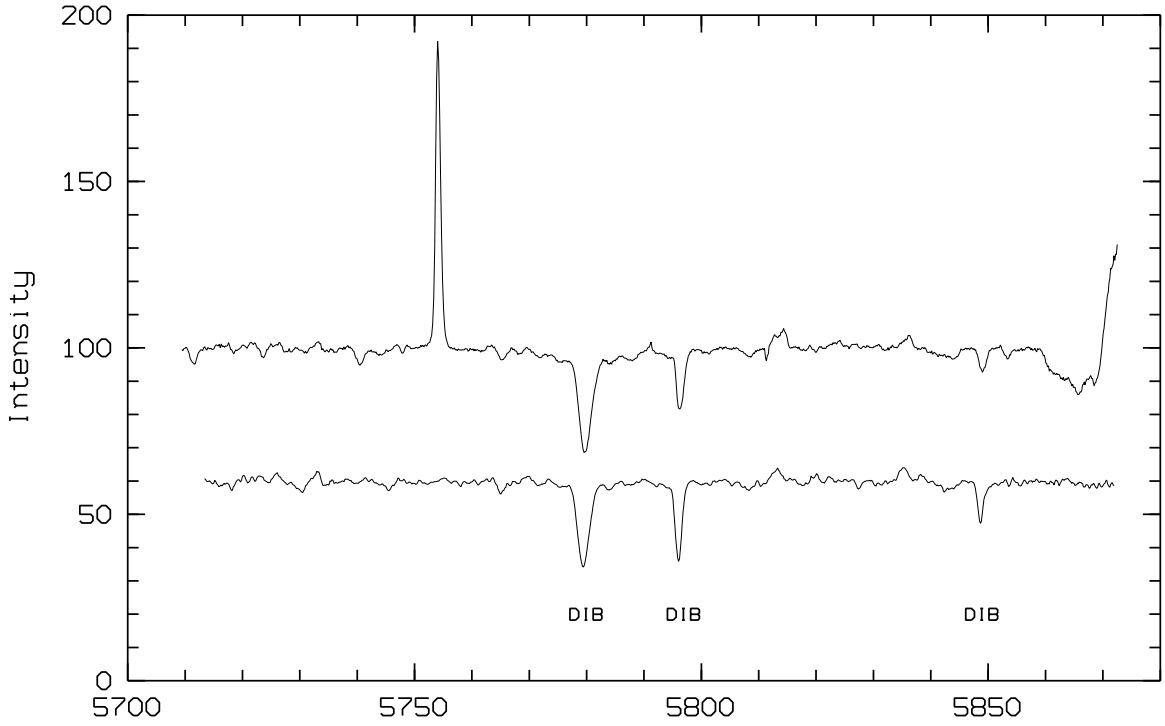

Figure 3.

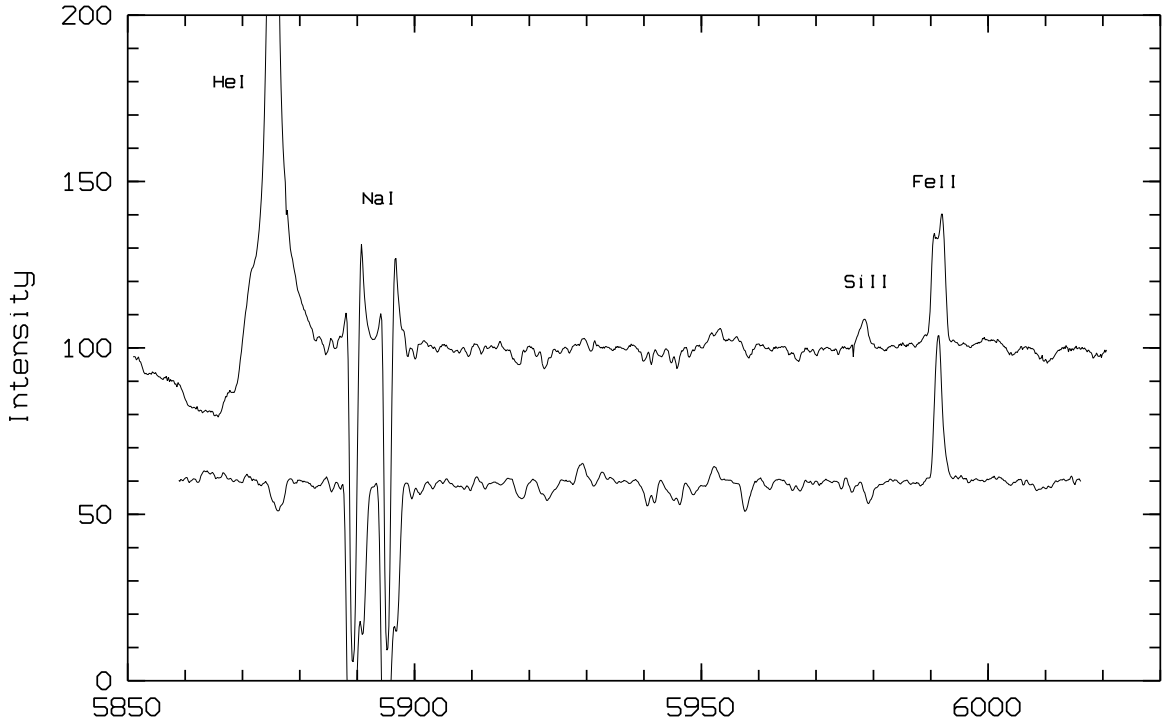

Figure 3.

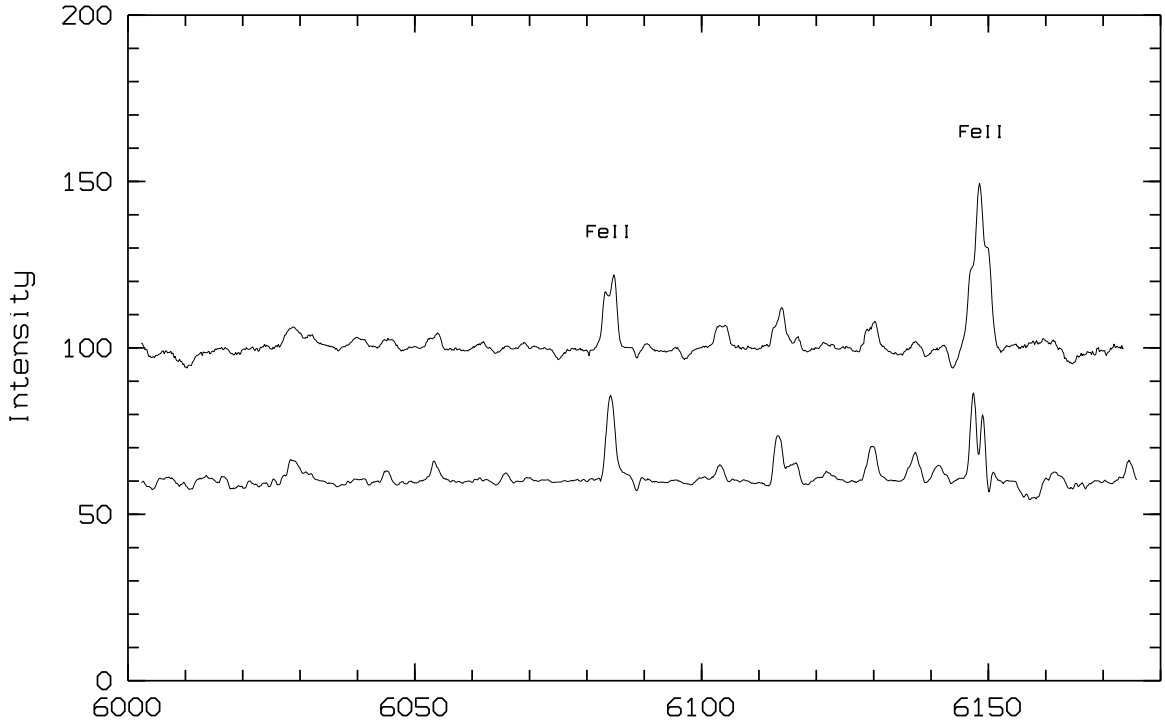

Figure 3.

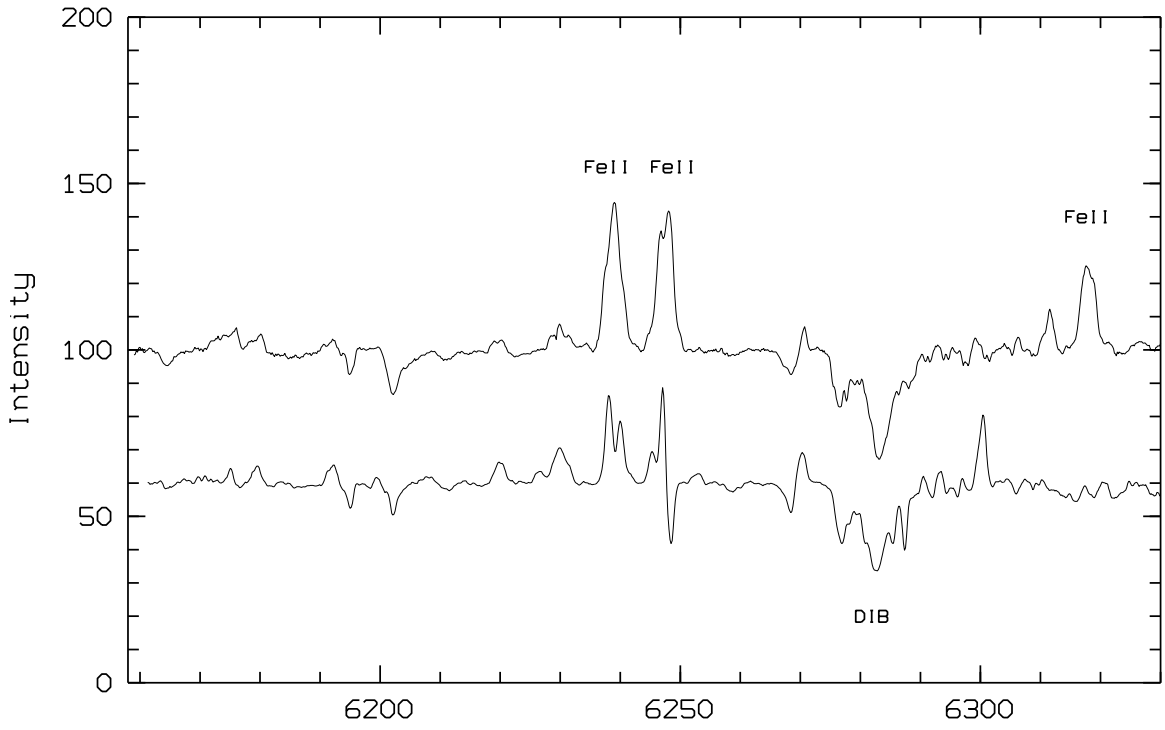

Figure 3.

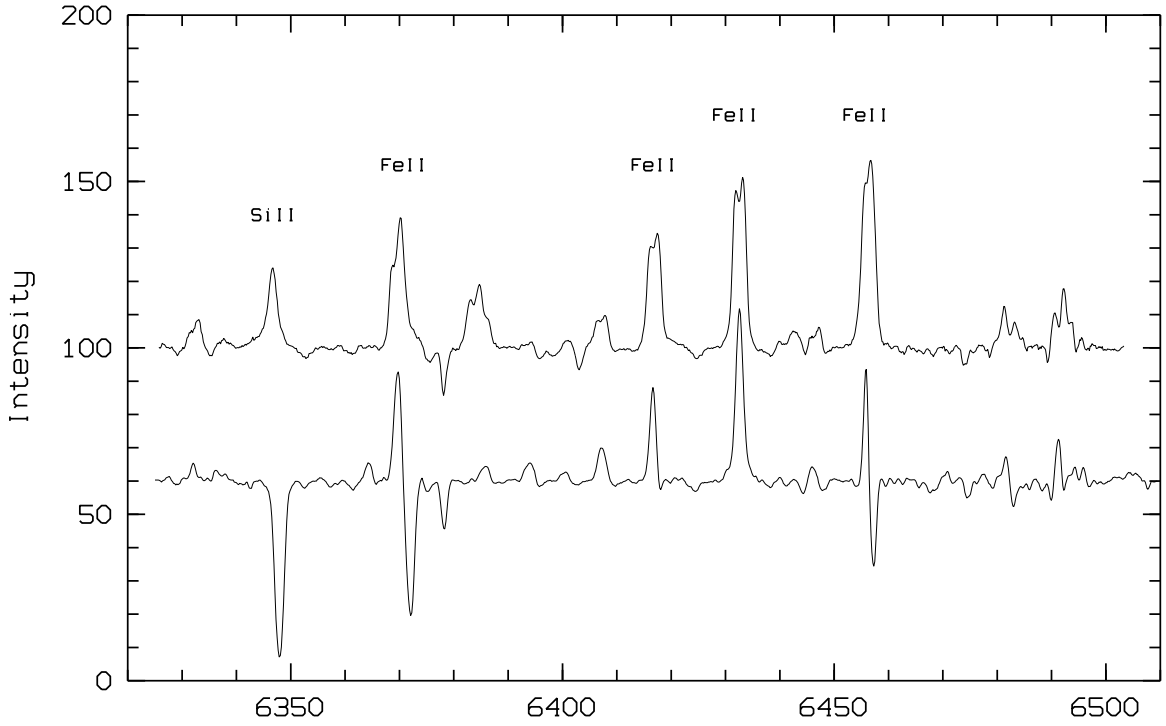

Figure 3.

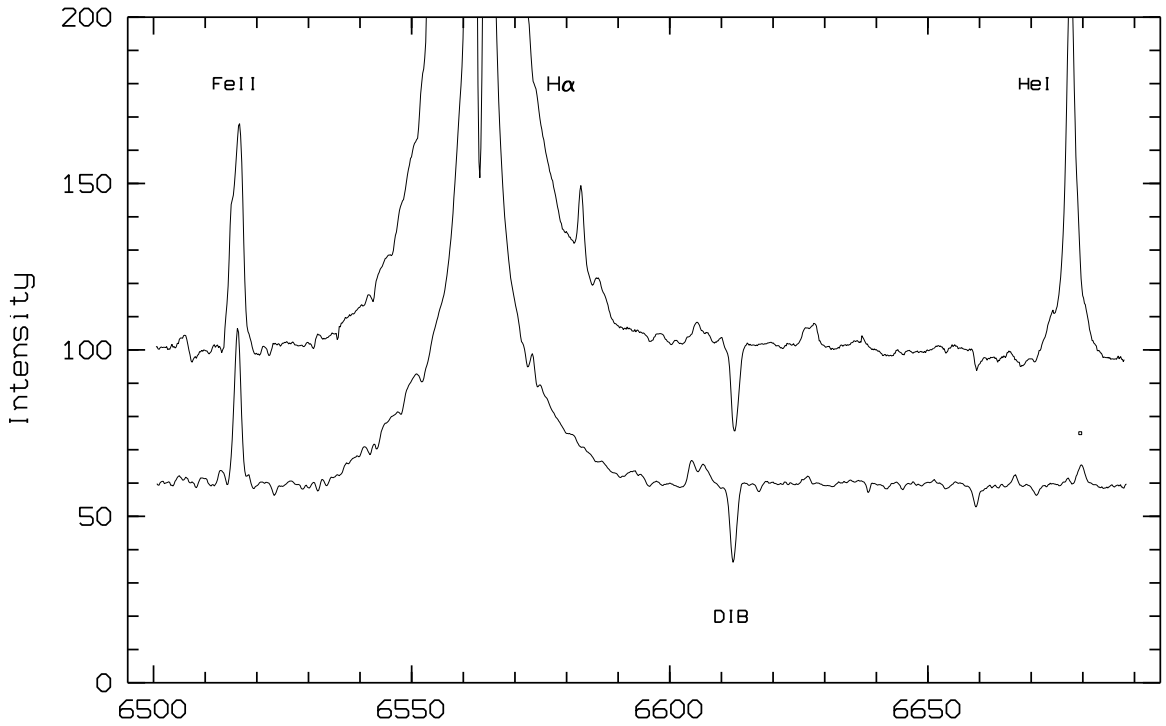

Figure 3.

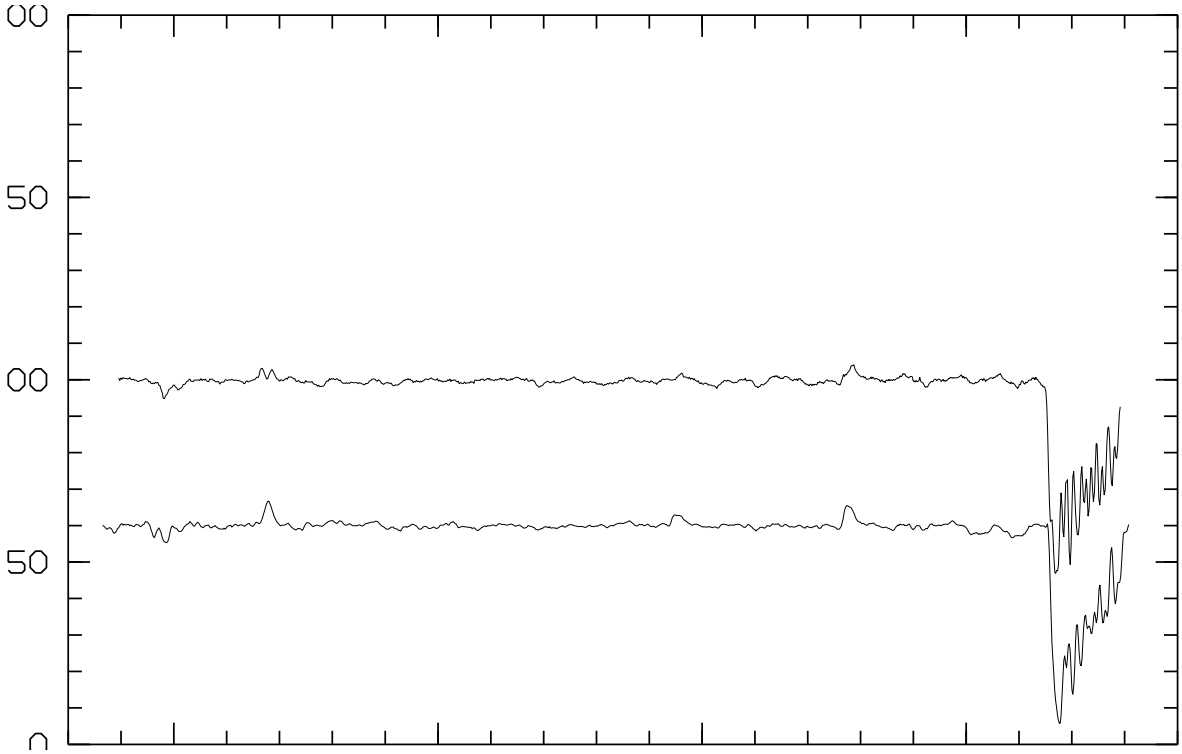

Figure 3.

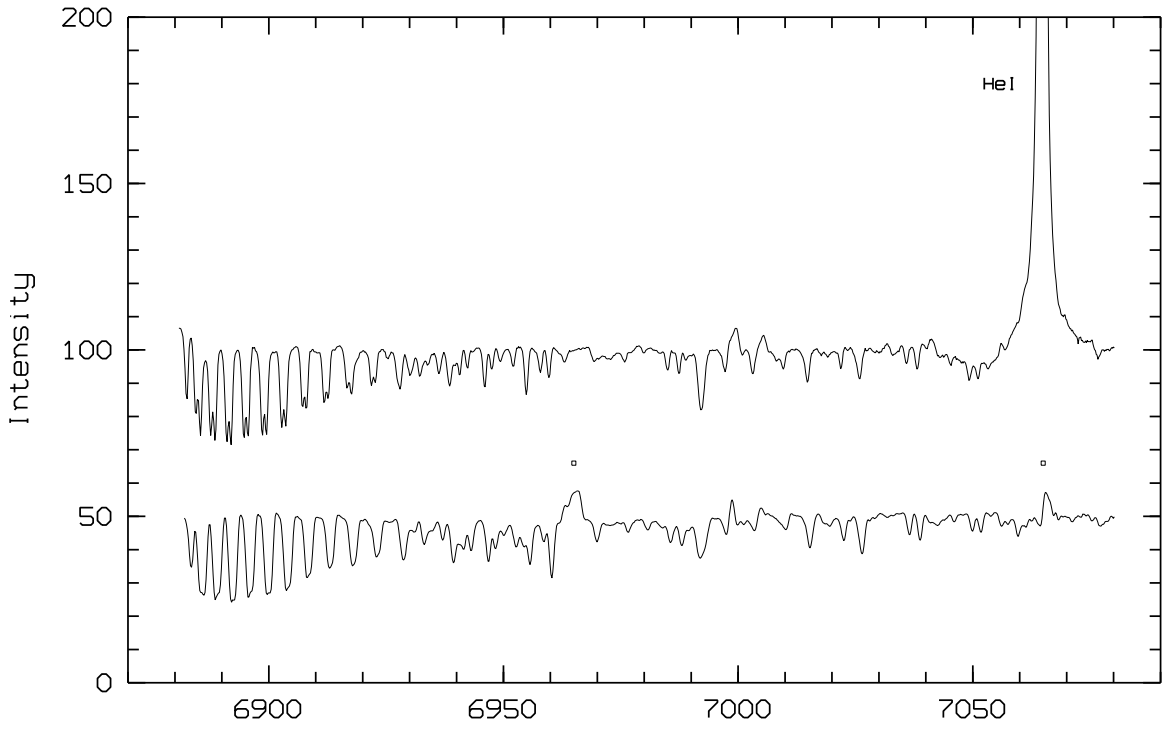

Figure 3.

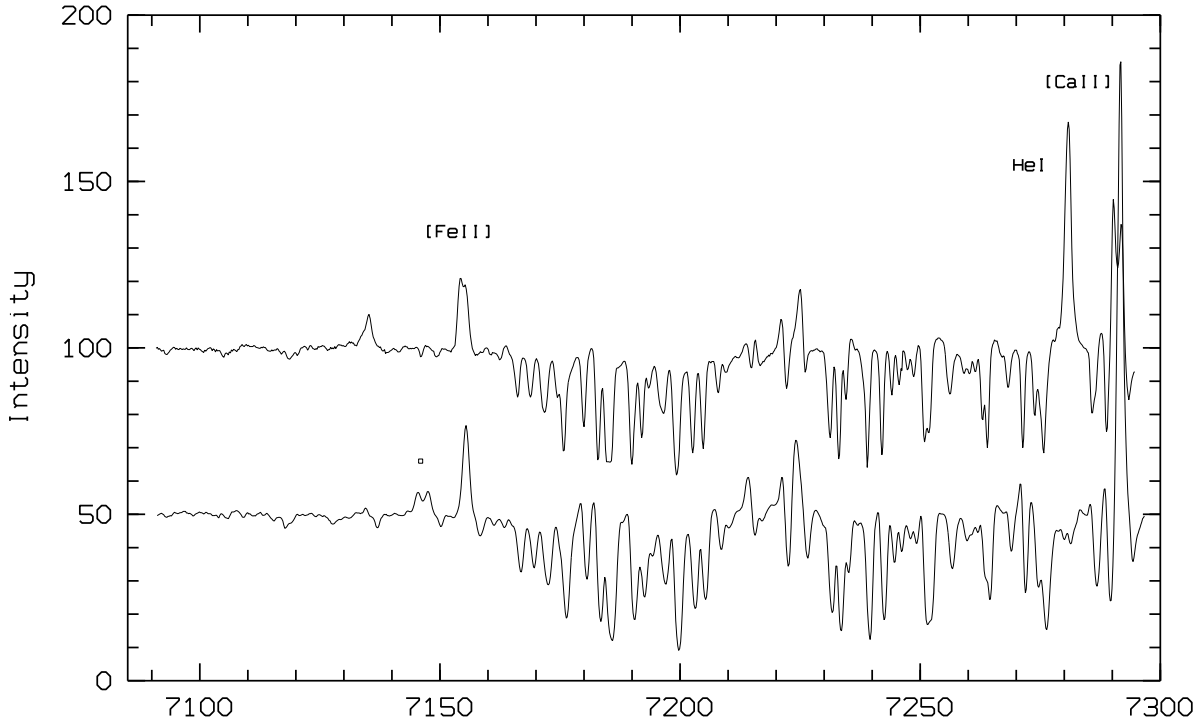

Figure 3.

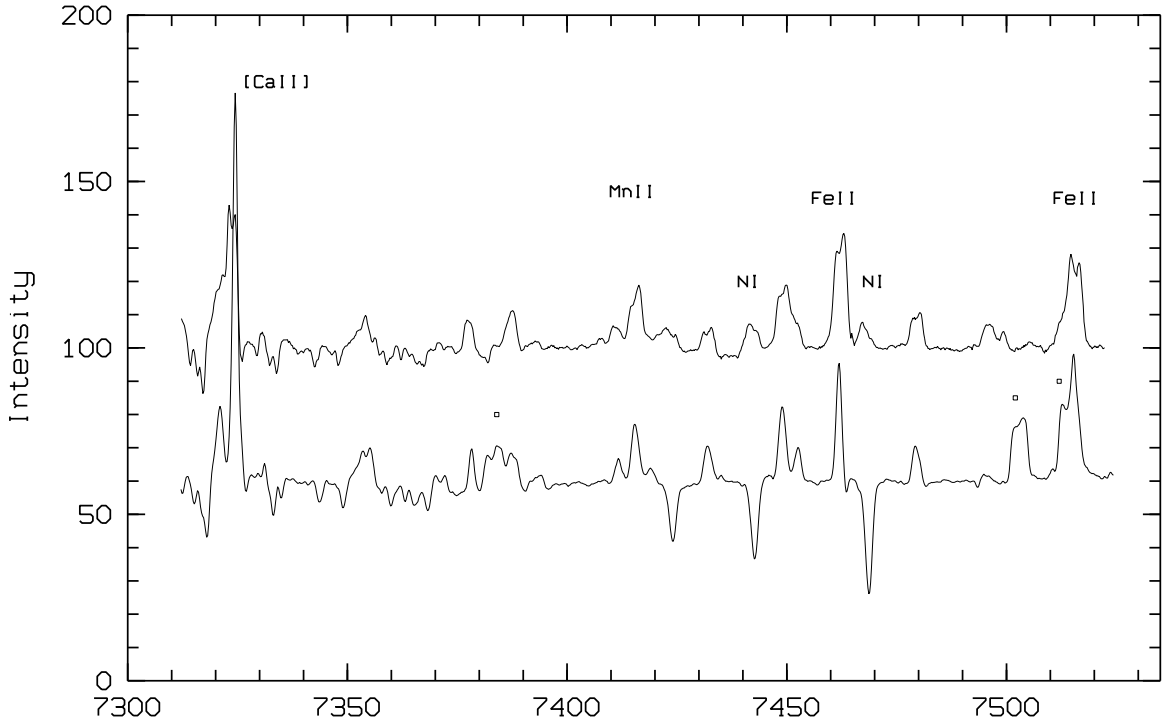

Figure 3.